



NUMERICAL FLOW SIMULATION

ME - 474

BC BUILDING ENTRANCE



Groupe 12:

AZEVEDO Sebastien - 282288 - sebastien.azevedo@epfl.ch

CANOEN Louis - 312526 - louis.canoen@epfl.ch

GRIFFON Pierre - 316216 - pierre.griffon@epfl.ch

KARAPAS Kleon - 315584 - kleon.karapas@epfl.ch

Professor:

BOUJO Edouard

Abstract

This study investigates the impact of door configurations on temperature regulation and heat loss within the BC building during winter. Two scenarios were analyzed: consecutive door openings and a diagonal door configuration, the latter being imposed during colder months to limit the influx of cold air. The primary objective was to assess whether the choice of door configuration significantly affects the average interior temperature and overall thermal efficiency.

Numerical flow simulations were conducted using ANSYS Fluent, employing a transient solver to capture airflow dynamics and temperature evolution over a 10-second time frame. The physical model assumes air as an incompressible Newtonian fluid, with density variations modeled using the ideal gas law to account for buoyancy effects. The simulation setup included a structured Cartesian mesh, refined in regions with significant gradients, such as door edges and high-shear zones. Three mesh levels, coarse, fine, and super-fine, were tested to evaluate convergence and ensure numerical accuracy. The final mesh provided a balance between computational cost and precision, with localized refinement in critical areas to capture the effects of airflow and temperature variations accurately.

Boundary conditions were set to replicate realistic conditions: an external temperature of 0°C, an internal temperature of 20°C, and an incoming airflow velocity of 3 m/s. The turbulence model employed was the k-omega SST model, chosen for its robustness in capturing near-wall effects and thermal mixing. Key points of interest included the doorway connecting the airlock to the main hall, the midpoint of the main hall, and the exit doorway.

The results demonstrate significant differences between the two configurations. In the consecutive door scenario, cold air flows directly into the main hall, causing a rapid temperature drop to approximately 11°C at the midpoint within 10 seconds. Conversely, the diagonal configuration effectively impedes airflow, confining it to the entrance hall and resulting in a slower and less severe temperature decline, stabilizing at 16°C. These findings highlight the diagonal configuration's ability to mitigate heat loss and maintain a higher interior temperature.

By incorporating detailed physical modeling, mesh refinement, and turbulence considerations, this study underscores the importance of simulation accuracy in assessing thermal performance. The results provide strong support for implementing diagonal doors in winter as an effective strategy to enhance energy efficiency and occupant comfort in public buildings.

Table of Contents

Abstract	1
1 Introduction	1
1.1 Context and goals of the study	1
1.2 Type of analysis, Methodology	1
2 Geometric modeling and hypotheses	2
2.1 Presentation of the geometry	2
2.2 Unit system	3
2.3 Characteristic dimensions	4
2.4 Symmetry, Periodicity and Geometrical space	4
3 Physical modeling and hypotheses	4
3.1 Physical behavior	4
3.2 Fluid properties	5
3.3 Turbulence model	5
4 Boundary conditions, external forces, initial conditions	7
4.1 Boundary conditions	7
4.2 External forces	7
4.3 Initial conditions	7
5 Computational mesh	8
5.1 Mesh type	8
5.2 Cell type	8
5.3 Size / number of cells	9
5.4 Final mesh	9
6 Numerical methods	10
6.1 Spatial discretization method	10
6.2 Type of simulation/solver	10
6.3 Solution options	12
6.4 Computed quantities	13

7	Mesh size / domain size convergence study	14
7.1	Criterion	14
7.2	Presentation of the different meshes	14
7.3	Results on the coarsest mesh	16
7.4	Results on the finest mesh	16
7.5	Estimation of the relative error	17
7.6	Precision of the temperature	17
7.7	Choice of the mesh / domain	18
8	Results	18
8.1	Case 1 : Consecutive doors	19
8.2	Case 2 : Diagonal doors.	22
9	Analysis & conclusions	25
9.1	Summary of calculated results	25
9.2	Relevance / accuracy of the results?	25
9.2.1	Comment on the minimum temperature	25
9.3	Conclusion	26
9.4	Recommendations	27
	Appendix	28

1 Introduction

1.1 Context and goals of the study

The BC building located at the EPFL campus has an airlock (entrance hall) to limit heat loss when doors are opened. There are two ways of accessing the interior of the building: through two consecutive doors (red line) or by zigzagging through two staggered doors (blue line), an option imposed in winter. This raises the following question :

Does the choice of door opening have a real impact on temperature and heat loss inside the building?



Figure 1: Entrance of the BC building.

1.2 Type of analysis, Methodology

To simulate the chosen study cases accurately, a detailed analysis of the real-life geometry and conditions is essential. The entrance hall features four doors, as illustrated in Figure 1. Two entry configurations are possible: either two consecutive doors open (one directly in front of the other) or the user must follow a diagonal path by opening the left door followed by the right, or vice versa. The diagonal configuration is enforced during the winter months. The key question is whether this diagonal arrangement has a significant impact on the average temperature inside the building. The simulation studies the passage of one person coming from outside and entering the building. The two configurations studied are as follows:

1. Consecutive doors: represented by the red line in Figure 1.
2. Diagonal path: represented by the blue line in Figure 1.

To define the physical model, the geometrical properties of the building were carefully measured using AR technology present in the *Measure* application on iOS and reported on figure 2. As for the physical conditions, the values were recorded on a normal December day. The average wind speed of 3 m/s and air temperature of 0°C were taken from the local weather app and the static temperature of the air inside the building being equal to 20°C was taken from a thermostat. The air blowing inside the entrance hall is assumed to be perfectly normal to the door surface.

2 Geometric modeling and hypotheses

2.1 Presentation of the geometry

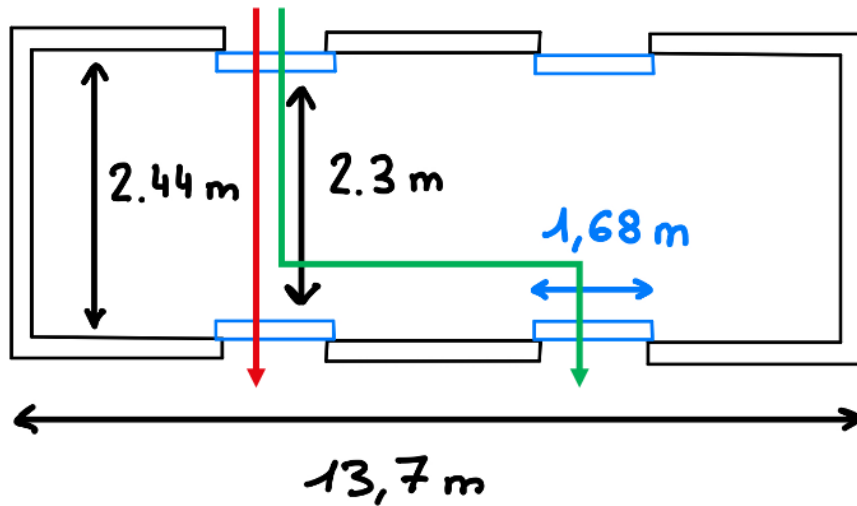


Figure 2: Sketch of the model : straight path (red), diagonal (green), doors (blue).

The airlock features a simple rectangular geometry measuring $13.7 \text{ m} \times 2.44 \text{ m}$. The full setup includes the airlock, as illustrated in Figure 2, and the main hall of the BC building, depicted in Figure 3. This case study focuses on three key points of interest: the doorway connecting the airlock to the main hall, the doorway between the exit hall and the main hall, and the midpoint between these two doorways, located at the center of the BC main hall.

Adding the main hall to the entrance hall allows us to study the effect of the door configuration on the rate of change of the temperature inside the building. The hallway in the back on the building serves as the pressure-outlet for the simulation. It was purposeful left long to help the incoming flow develop completely before reaching the outlet of the domain.

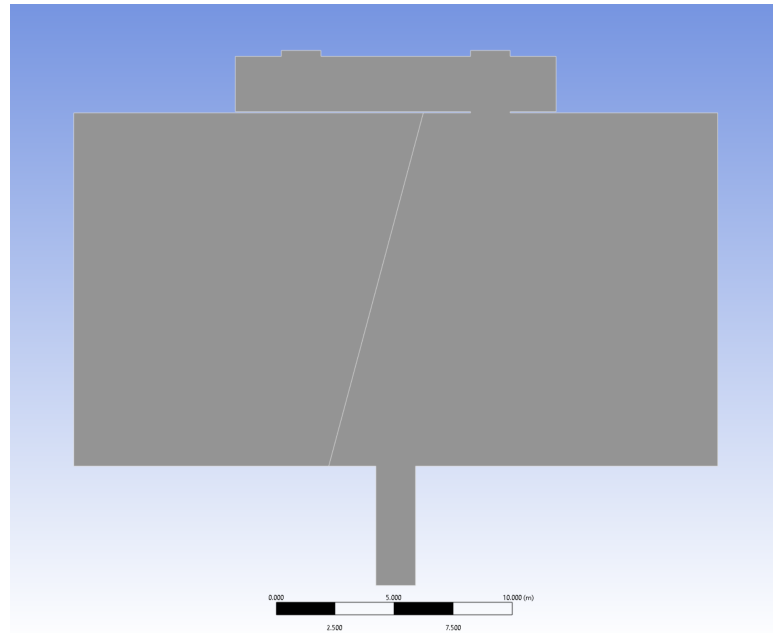


Figure 3: 2D modeling of the building entrance.

2.2 Unit system

The International System is used as the unit system used in this study, except for the temperature where both Celsius and Kelvins are used interchangeably depending on the relevance. The temperature boundary and initial conditions were defined in Celsius while the other physical quantities involving temperature were left in Kelvin.

Dimension	Unit	Symbol
Length	meter	m
Time	second	s
Temperature	Celsius/Kelvin	°C / K
Weight	kilogram	kg
Amount of substance	mole	mol

Table 1: Unit System used.

2.3 Characteristic dimensions

Category	Characteristic Dimension
Airlock Geometry	<ul style="list-style-type: none"> - Width of each door - Distance between consecutive doors - Offset distance between staggered doors
Building Interior and Exterior	<ul style="list-style-type: none"> - Interior height adjacent to the airlock - Outdoor temperature variation
Door Dynamics	<ul style="list-style-type: none"> - Opening width of each door - Opening/closing duration - Frequency of door use
Thermal Properties	<ul style="list-style-type: none"> - Temperature difference (interior vs. exterior) - Air exchange area per door opening
Air Movement	<ul style="list-style-type: none"> - Airflow rate through the doors - Pressure differential across the airlock

Table 2: Characteristic Dimensions for 2D Airlock Heat Loss Analysis.

2.4 Symmetry, Periodicity and Geometrical space

Geometrically, the airlock and surrounding building structure can be assumed to have a horizontal planar symmetry, allowing for a 2D approximation of the system. This means that variations in the vertical (z) direction are negligible compared to the x - y plane, which includes the width and height of the airlock. This means that gravity and its underlying effects are ignored during this study.

In terms of boundary conditions, the flow of air through the doors and the heat exchange are symmetric across the vertical midline of the airlock when both consecutive and staggered doors are considered.

External forces, such as wind, introduces asymmetry, particularly if it acts predominantly on one of the two entrances. However, in a controlled environment or for simplification, the effect of wind can be considered uniform for both external doors.

This symmetry in geometry and boundary conditions aids in reducing the computational domain and simplifies the numerical model.

3 Physical modeling and hypotheses

3.1 Physical behavior

The only fluid considered in this study is air. It is treated as incompressible because the maximum Mach number Ma , remains well below 0.3 (calculated later). This assumption significantly simplifies the model by reducing the number of governing equations for the physical system.

Air is also modeled as a Newtonian isotropic fluid, as its viscosity is independent of the shear rate. Additionally, the ideal gas law is applied since the physical properties of the problem fall within its valid range. This is justified by factors such as atmospheric pressure, temperatures near standard conditions, and the relative size of the building, which renders molecular interactions negligible. The ideal gas law is particularly useful for determining properties like density.

Given that the fluid will experience non-negligible temperature differences, heat energy transfer is included in the modeling. These temperature variations can alter the air density, leading to buoyancy effects that influence the system's behavior.

Finally, phase changes and combustion are not considered in this study, as the air remains in a single phase and no chemical reactions occur.

3.2 Fluid properties

Property	Value (at 20°C)
Density [kg/m ³]	1.204
Cp (specific heat) [J/(kg · K)]	1006.43
Thermal conductivity [W/(m · K)]	0.02514
Viscosity [kg/(m · s)]	1.7894 · 10 ⁻⁵

Table 3: Fluid Properties of Air.

The temperature range extends from 0°C (cold air outside the room) to 20°C (hot air inside), and the ideal gas model is employed to account for the temperature variation as discussed in 3.1. The specific heat varies by only 1 J, which is negligible, and is thus assumed constant throughout the process, while the thermal conductivity increases slightly by three percent, a variation also deemed negligible. However, viscosity increases by 8%, which is significant; therefore, it is modeled using a linear interpolation based on values at 0°C and 20°C. The properties are summarized in the Table 3.

3.3 Turbulence model

Considering that the order of magnitude of the building is 10¹ [m], the range of Reynold's number observed will be way beyond the laminar-turbulent transition. A turbulence model is thus needed.

The turbulence model used in our simulation is the k-omega (k- ω) turbulence model. This model is well-known for capturing correctly near-wall effects and dealing with thermal airflow mixing, which are key physical phenomena in this study. In contrast, models such as the k-epsilon (k- ϵ) turbulence model may not be well suited as it is less robust in low-Re regions such as the mixing regions where the cold air mixed with the warm still air.

The turbulence kinetic energy k and the specific dissipation rate ω are obtained from the following transport equations:

$$\frac{\partial}{\partial t}(\rho k) + \frac{\partial}{\partial x_i}(\rho k u_i) = \frac{\partial}{\partial x_j} \left(\Gamma_k \frac{\partial k}{\partial x_j} \right) + G_k - Y_k + S_k + G_b \quad (1)$$

$$\text{and } \frac{\partial}{\partial t}(\rho \omega) + \frac{\partial}{\partial x_i}(\rho \omega u_i) = \frac{\partial}{\partial x_j} \left(\Gamma_\omega \frac{\partial \omega}{\partial x_j} \right) + G_\omega - Y_\omega + S_\omega + G_{\omega b} \quad (2)$$

In these equations, G_k represents the generation of turbulence kinetic energy due to mean velocity gradients. G_ω represents the generation of ω . Γ_k and Γ_ω represent the effective diffusivity of k and ω , respectively. Y_k and Y_ω represent the dissipation of k and ω due to turbulence. All of the above terms are calculated as described below. S_k and S_ω are user-defined source terms. G_b and $G_{\omega b}$ account for buoyancy terms as described in *Effects of Buoyancy on Turbulence in the k- ω Models* (p. 69).

When selecting this turbulence model, many solver options are available:

- **k- ω model:** The SST (Shear Stress Transport) model is an appropriate choice for flows involving separation, recirculation, and boundary layer interactions, such as those near sharp 90-degree corners, making it advisable to retain the "k-omega" and "SST" options. The SST model incorporates all the refinements of the BSL model and further accounts for the transport of turbulence shear stress in defining turbulent viscosity, enhancing its accuracy and reliability for a broader range of flows, including those with adverse pressure gradients, airfoils, and transonic shock waves.
- **Low-Re correction:** For simulations involving relatively low Reynolds numbers or where accurate near-wall behavior is critical, enabling this option is recommended. However, for high-Reynolds-number flows, such as those typical in building-scale simulations, this feature may not be necessary.
- **Viscous heating:** Likely unnecessary unless there is significant heating due to viscous dissipation, which isn't expected in this case.
- **Curvature control:** Not needed unless there are curved surfaces influencing the flow, which isn't applicable to our building composed of 90-degree corners.
- **Corner Flow Correction:** May not be necessary as it's usually used for specific corner flow modeling.
- **Compressibility Effects:** This option should be disabled unless the simulation involves high-speed compressible flows (e.g., Mach numbers near or exceeding 0.3), which is not applicable to this study, as the Mach number is well below 0.3.
- **Production Kato-Launder:** This option should be disabled unless the simulation involves significant streamline curvature, which is not applicable to the current building simulation.
- **Production Limiter:** This option should remain enabled to prevent excessive turbulence generation, particularly in regions with sharp gradients, such as the corners of the building.

Only the Production Limiter solver options was enabled.

4 Boundary conditions, external forces, initial conditions

4.1 Boundary conditions

The boundary conditions relating to this specific case study are listed in the table below :

Boundary conditions	
Inlet boundary	
Velocity inlet [m/s]	3
Temperature [°C]	0
Outlet boundary	
Static pressure [Pa]	101'325
Temperature [°C]	20
Wall boundary	
Type	No slip
Wall temperature [°C]	20
Heat flux [kg/(m.s)]	1006.43

Table 4: Case study boundary conditions.

Heat transfer through the walls is not considered in this case study, as its influence is negligible over the short time frame analyzed. The focus of the simulation is on the immediate impact of airflow and temperature variations caused by door openings, which are the primary factors affecting the interior temperature during this period. Furthermore, the walls of the building are presumed to be well-insulated, minimizing any significant heat exchange. By excluding wall heat transfer, the model is simplified without compromising the accuracy of the analysis regarding the effects of airflow and door configurations.

4.2 External forces

External forces, such as gravity, were not considered in this analysis, as the study is conducted in a 2D horizontal plane and gravity effects are negligible in this context.

4.3 Initial conditions

The initial conditions relating to this specific case study are listed in the table below :

Initial conditions	
Temperature distribution	
Initial building temperature [°C]	20
Initial wall temperature [°C]	20
Initial outside temperature [°C]	0
Airflow condition	
Initial incoming airflow velocity [m/s]	3
Initial interior airflow velocity [m/s]	0
Pressure	
Interior initial pressure [Pa]	Atmospheric pressure

Table 5: Case study initial conditions.

The initial conditions were selected to replicate a realistic scenario for the BC building during winter. An exterior temperature of 0°C was assumed to reflect typical seasonal conditions, while the interior temperature was set to 20°C, representing a heated indoor environment. These conditions allow for a meaningful analysis of the temperature drop and airflow behavior when doors are opened, ensuring the simulation captures the key dynamics relevant to the case study.

5 Computational mesh

5.1 Mesh type

In our case we used a structured mesh, more precisely a cartesian grid as it is easy to generate and suits well the simple geometry of the room. We used three different meshes in order to compare their performance, with the exact same geometry but with finer cells each time (see Section 7 for a more detailed account of the three meshes).

5.2 Cell type

Since the building is made of rectangles with right corners, most of the elements of the mesh are quadrilateral. To increase precision, all elements are quadratic type.

After preliminary simulations to identify regions with minimal change (e.g., the "B" region on the left side of the main hall), it was found that the "B" region saw almost no change after 10 seconds. To reduce computation, this region was separated from the main region of interest ("A" region) by a diagonal line starting 2 meters from the left extremity of the doors (see Figure 3) and assigned a larger local mesh size. The dividing line caused some elements to remain as triangles instead of being converted to quadrilaterals to accommodate the different angle.

5.3 Size / number of cells

For the coarse mesh we have a total of 9813 elements and 30136 nodes and for the super-fine mesh 108424 elements and 327151 nodes.

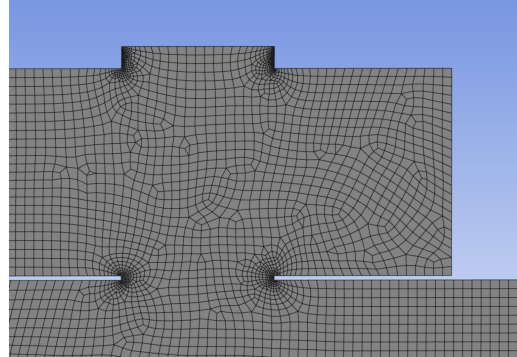


Figure 4: Local mesh refinement at the entries.

At the edges of the doors, boundary layer effects must be taken into account, as velocity and temperature gradients must be high. One important effect that we noticed near the door edges, was a vortex formation due to the sudden change in geometry and therefore a finer mesh is needed to accurately represent the flow structure at these points. As seen in Figure 4, at the corners we have elements that are 1/10 of the size of the regular cells (see Table 6).

5.4 Final mesh

The following Figure 5 depicts the mesh structure that we chose to use for our study. A diagonal cut with larger elements is placed on the left side because this part of the room experiences quasi-minimal variations in flow or thermal gradients. By using coarser elements in this region, we efficiently reduce the total number of cells, thereby saving computational resources. We also proceeded to a mesh refinement at the edges of the outlet for the same reasons as mentioned before.

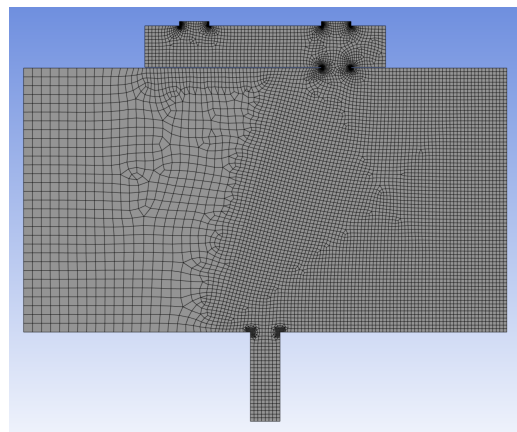


Figure 5: Final mesh structure.

6 Numerical methods

6.1 Spatial discretization method

Fluent primarily uses the finite-volume method (FVM) for spatial discretization. The interpolation scheme chosen was QUICK, as it is a higher-order scheme that is well adapted for convection-dominant flows. As we are in the transient case, a second-order implicit scheme was used, which in Fluent corresponds to the Backward Differentiation Formula (BDF) of second order:

$$\frac{3T^{n+1} - 4T^n + T^{n-1}}{\Delta t}$$

One disadvantage of BDF is that while it allows for better accuracy compared to a first-order scheme it may produce oscillations (see *Lecture: Time integration of NFS*) which is visible in Figures 26a and 26.

6.2 Type of simulation/solver

As we are interested in studying a transient problem, a transient simulation is used. The simulation employs a pressure-based problem as density-based simulation are more used in problems where compressibility is more prevalent than in our case. The general Mach number Ma is below the threshold where compressibility cannot be ignored ($Ma \approx 10^{-3} \ll 0.3$). In our case density change due to pressure gradients can be ignored.

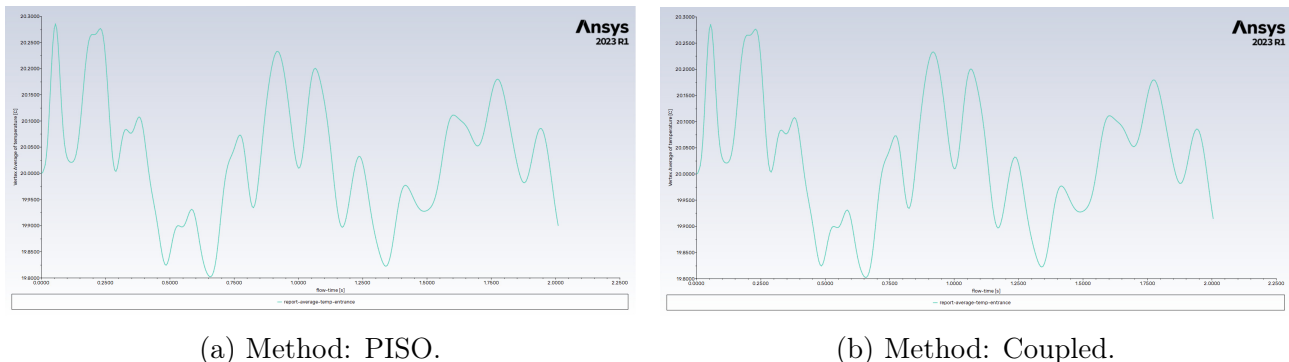


Figure 6: Local temperature at the entrance point with respect to time.

As shown in Figure 6, the difference between the "PISO" and "Coupled" methods is negligible. Although the Coupled method requires 1.5-2 times more memory and slightly more time per iteration, it generally converges in 30% fewer iterations than PISO, resulting in similar overall simulation times for both methods. Since the computer used for this simulation can handle the increased memory requirement, the Coupled method was chosen.

The governing equations of our system are the following:

$$\begin{cases} \nabla \cdot \mathbf{u} = 0 \\ \rho \frac{\partial \mathbf{u}}{\partial t} + \rho(\mathbf{u} \cdot \nabla) \mathbf{u} = -\nabla p + \mu \nabla^2 \mathbf{u}, \\ \rho c_p \frac{\partial T}{\partial t} + \rho c_p (\mathbf{u} \cdot \nabla T) = \nabla \cdot (k \nabla T). \end{cases}$$

Here the first two are the Navier-Stokes equations (continuity and momentum respectively) and the third is the energy equation for temperature, which links it to the flow fields via convective terms $\mathbf{u} \cdot \nabla T$.

Both cases were modeled and analyzed using ANSYS Fluent with the simulation settings detailed below:

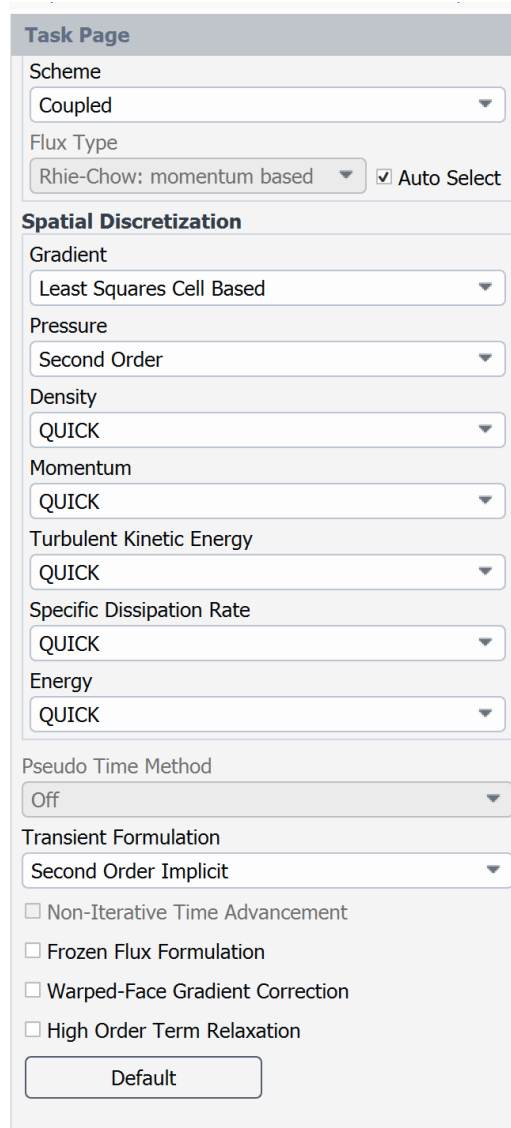


Figure 7: Simulation method settings.

6.3 Solution options

We use the standard method as opposed to the hybrid method to solve our transient problem. Since we have prior knowledge of the initial flow field and of the initial conditions, the hybrid method would be unnecessary and overly complicated.

Criteria for convergence used when solving (these are the default values for the residuals that were left untouched):

- continuity: 1e-3
- x-velocity: 1e-3
- y-velocity: 1e-3
- energy: 1e-6
- k: 1e-3
- omega: 1e-3

For fixed time step size using an explicit time scheme, we normally should choose Δt to satisfy the Courant-Friedrichs-Lowy (CFL) condition:

$$\Delta t < \frac{\min(\Delta x)}{\max(U)} \quad (3)$$

where, Δx is the size of the elements of a local mesh and U is the magnitude of the speed at any given point in the domain.

However, this condition is rather limiting. To remedy that, we can use a second-order implicit time scheme to lift this condition and have more freedom. In the solver, we can choose to have an adaptive time step based on the CFL condition. The solver will automatically adapt Δt to satisfy the new CFL condition based on the Courant Number C :

$$C = \frac{U \Delta t}{\Delta x} \leq C_{\max} \quad (4)$$

where C_{\max} should be strictly smaller than 1 for explicit time scheme but can be smaller than 1 for implicit time scheme. Choosing a larger value C_{\max} will increase Δt , but can cause instability if the value is too large.

However, the time steps were too reasonably small for our simulation after doing some testing with a second-order implicit time scheme and adaptive time steps. The time steps were around 10^{-5} s in magnitude, with C_{\max} values ranging between 1 and 100. If the solver took about 1 second to compute one time step, simulating 10 seconds would take 11 and a half days which is not ideal. For academic purposes, three time steps Δt were chosen to study their impact on the final results.

As for the maximum number of iterations allowed per time step, it was increased from 20 (default value) to 100 in order to face any possibility. As a matter of fact, the number of iterations per time step never exceeded 20 in practice.

- Temporal time scheme: second-order implicit
- Global time step Δt : 0.05 s, 0.01 s and 0.005 s
- Maximum number of iterations allowed: 100

6.4 Computed quantities

In this study, temperature of absolute velocity are the main two quantities of interest. The temperature is important to monitor the impact of the cold air rushing inside the building while the velocity is useful to compare both cases (parallel vs diagonal cases). In particular, the temperature is measured at three different points inside the building:

- **Entrance - point:** Located at the junction between the entrance and the main hall, the entrance-point monitors the rate at which cold air transitions between the two rooms.
- **Outlet - point:** Situated at the boundary between the main hall and the hallway, the outlet-point monitors the movement of cold air away from the building's entrance.
- **Midpoint:** Placed exactly at the geometric midpoint between the two previous points, the midpoint studies the impact of the cool wind around the middle of the main hall.

At these points, the average vertex temperature (in the nomenclature of Fluent) is monitored through time. Since the three points are never perfectly aligned with the nodes of the mesh, Fluent interpolates from the neighboring node values.

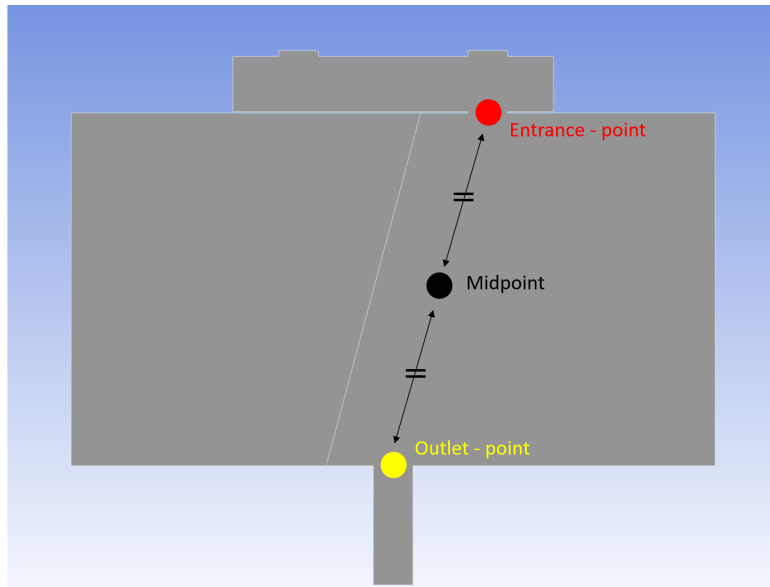


Figure 8: Illustration of the three points of interest where the local temperature is measured.

7 Mesh size / domain size convergence study

7.1 Criterion

Assessing convergence in this study is challenging because we cannot analyze a steady-state parameter like the lift coefficient; instead, in this transient study, computed quantities vary in space and time. Since we focus on a 10-second window rather than steady-state behavior, we select a specific point in the domain and a particular time as a reference for comparing different meshes, with a fixed time step $\Delta t = 0.005\text{ s}$ for the convergence criterion.

To analyze mesh convergence, we will examine the temperature at the outlet point of the domain at $t = 10\text{ s}$. This point was chosen arbitrarily but provides a good indication of mesh consistency since it is located far from the entrance, and 10 seconds allows sufficient time for airflow differences between meshes to manifest.

7.2 Presentation of the different meshes

Name	El. size (A)	El. size (B)	El. size (special walls)	Nb. of elements
Coarse mesh	20 cm	50 cm	1 cm	9813
Super-fine mesh	5 cm	50 cm	1 cm	108424

Table 6: The three types of meshes used in the study.

Name	$\Delta t = 0.05\text{ s}$	$\Delta t = 0.01\text{ s}$	$\Delta t = 0.005\text{ s}$
Coarse mesh	2' 40"	13'	27'
Super-fine mesh	13'	1 h 5'	2 h 10'

Table 7: Total simulation time required for every case (10 seconds).

The general approach for generating the two meshes was to increase by ten folds the total number of elements. Only the local element in the "A" domain were decreased in size while keeping the "B" domain unchanged at 50 cm per element, as it does not undergo significant changes during the 10-second simulation. Refining to an element size smaller than 5 cm posed challenges due to software limitations caused by the high element count. As shown in Table 7, the total simulation time already exceeds 2 hours for the SuperFine mesh, which is a significant computational time. In this case, the marginal increase in precision does not justify the significant additional computational cost.

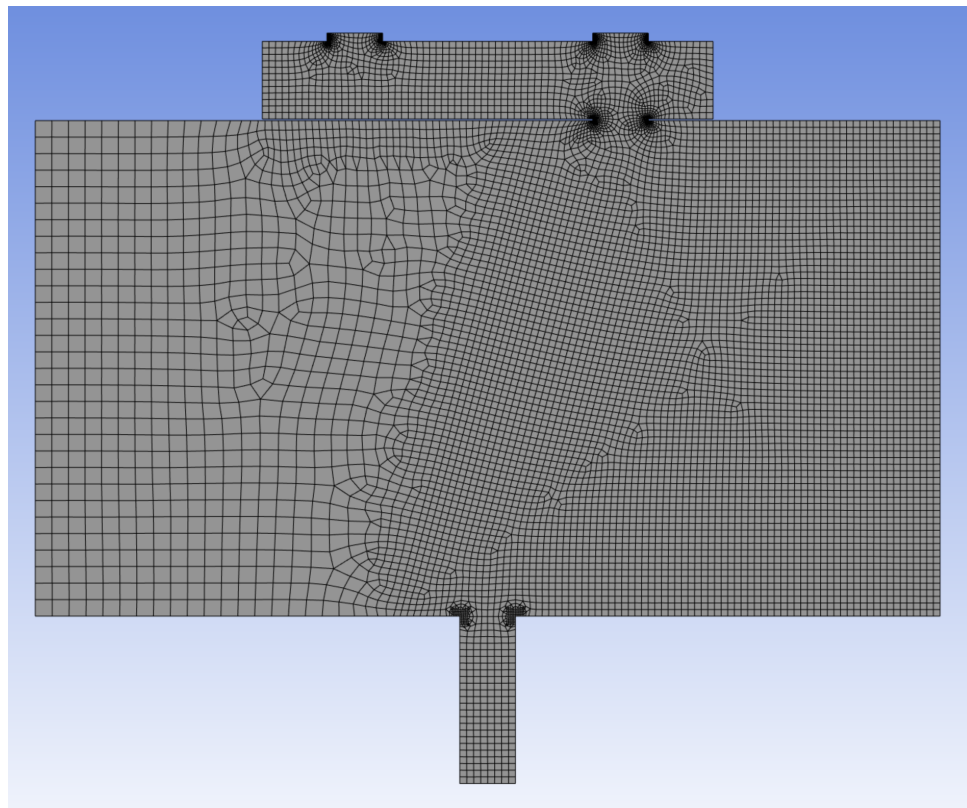


Figure 9: Illustration of the coarse mesh.

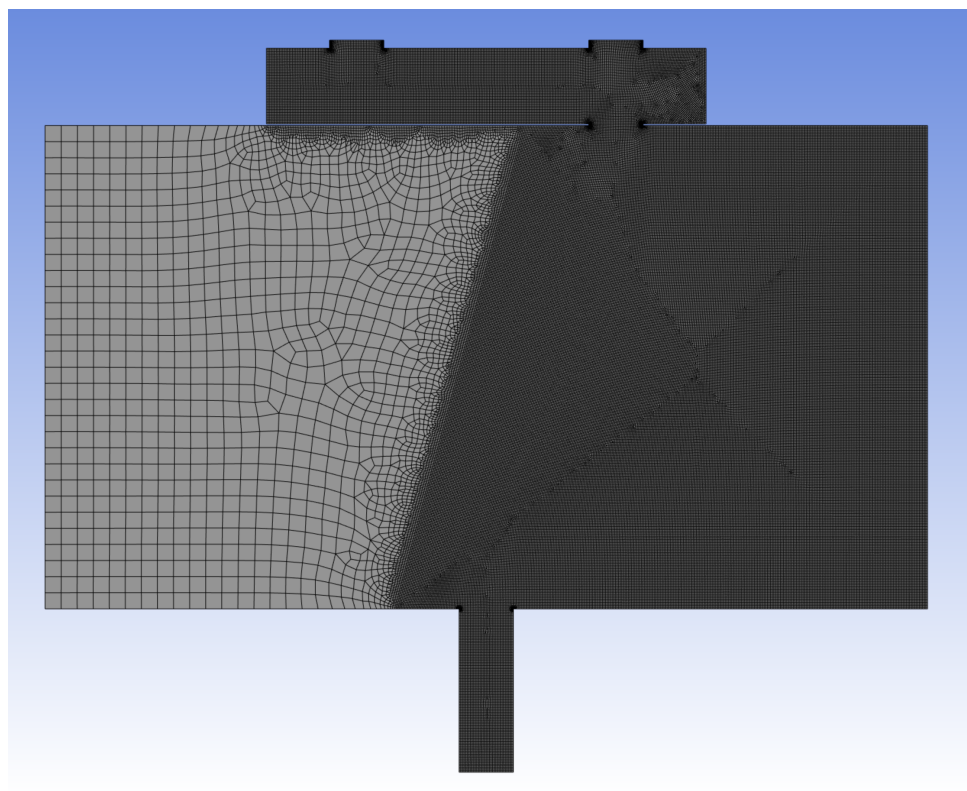


Figure 10: Illustration of the super-fine mesh.

7.3 Results on the coarsest mesh

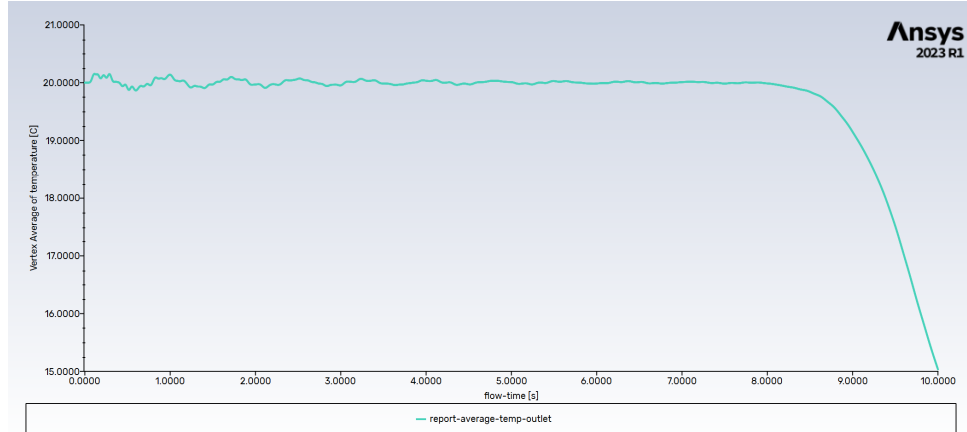


Figure 11: Evolution of the local temperature at the outlet point with respect to time on the coarse mesh ($\Delta t = 0.005$ s).

After 10 seconds have elapsed, the local temperature measured on the entrance point falls to 15.0282°C . We can observe some oscillations starting from the beginning of the simulation and gradually dampen out. This phenomena appears and is amplified when Δt decreases under a certain value.

7.4 Results on the finest mesh

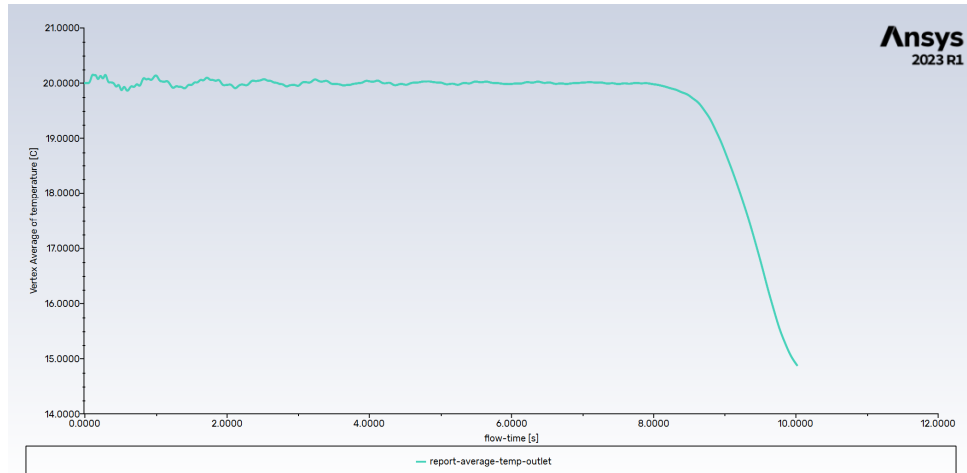


Figure 12: Evolution of the local temperature at the outlet point with respect to time on the super-fine mesh ($\Delta t = 0.005$ s).

After 10 seconds have elapsed, the local temperature measured on the entrance point falls to 14.8412°C .

7.5 Estimation of the relative error

When fixing the super-fine mesh as the reference mesh, we can compute the relative error made when using the coarse mesh:

$$\epsilon = \frac{T_{coarse} - T_{s.fine}}{T_{s.fine}} = \frac{15.0282 - 14.8412}{14.8412} = 1.26\% \quad (5)$$

This means that the user would make a 1.26% mistake by choosing the coarse mesh instead of the super-fine one. When considering the extra computation time required to complete the simulation with the super-fine mesh, the extra precision might become irrelevant. However, we need to remember that only a single point in a single time frame is being taken into account for the calculation of ϵ . Selecting the coarse mesh for studying the average temperature over a wide domain for instance, is more adapted than using the super-fine mesh.

7.6 Precision of the temperature

The temperature precision is not only dependent on the size of the mesh like in a steady-state problem. The time step Δt plays a big role in how the flow develops through time, thus affecting how the temperatures evolves throughout the region. As seen in Figure 13, increasing Δt reveals some finer detail that may have been damped with larger time steps. It seems that decreasing Δt may leave more time for the flow to develop finer structures such as small vortices. This smaller elements present on the boundary between the cold air flux and the still warm air are captured by the presence of higher temperature spikes especially on Figure 13b.

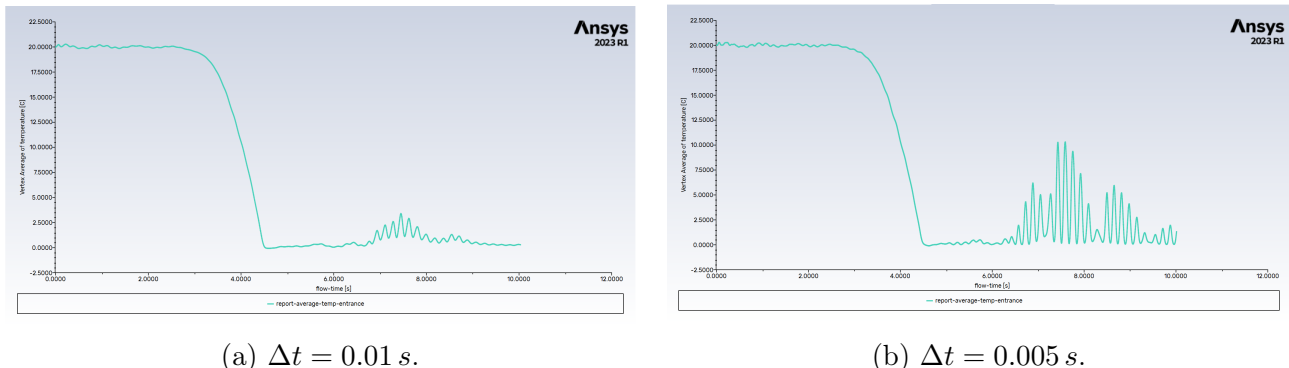


Figure 13: Impact of Δt on the precision of local temperature at the entrance point (super-fine mesh).

The behavior is also visible when decreasing the size of the mesh elements. The small vortices are created after the flow passes through the door between the entrance hall and the main hall between the period $t = [7\text{ s}, 10\text{ s}]$. This oscillations may appear due to the sudden expansion of the domain from the relatively confined entrance hall to the open main hall. As for a photograph, increasing the resolution of the simulation reveals these delicate structures which were lost or smoothed out with the coarse mesh. On Figure 14, the loss of detail of clearly present with the coarse mesh while the intricate vortices can more naturally develop thanks to the smaller elements of the mesh. The temperatures spikes observed between approximately 7

to 10 seconds at the entrance-point will be smaller with the coarse mesh than with the super-fine mesh. Working with a small Δt value is not the only sufficient condition to observe finer structures throughout an arbitrary mesh.

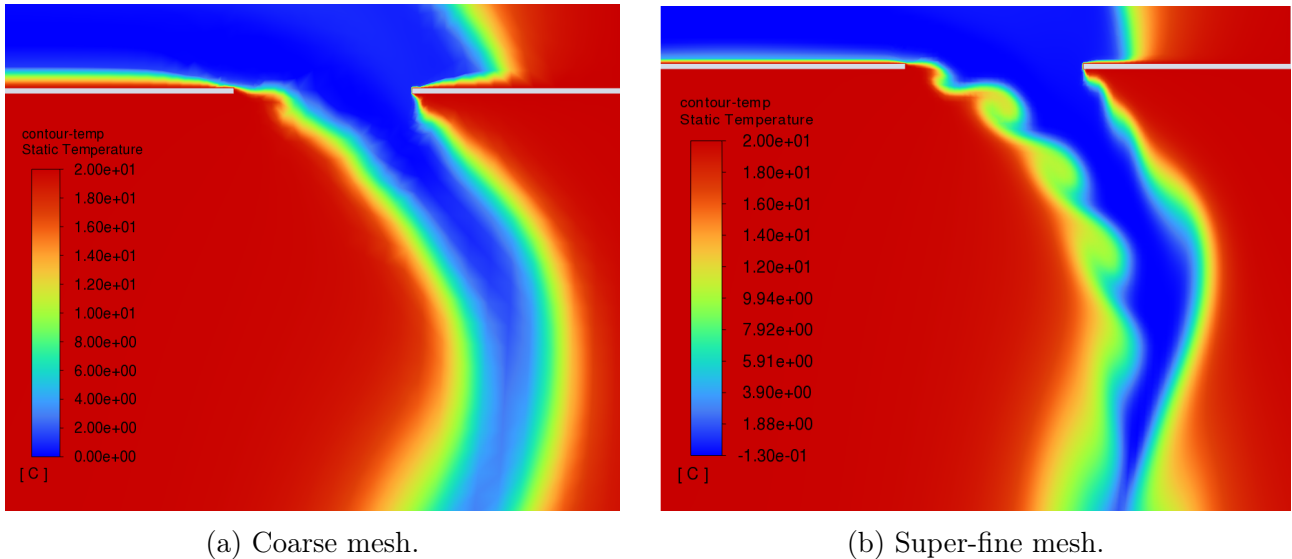


Figure 14: Impact of the mesh size on the shape of the airflow ($\Delta t = 0.005 \text{ s}$, $t = 7.5 \text{ s}$).

7.7 Choice of the mesh / domain

The choice of the mesh used greatly depends on what the goal of the study is. In order to study the temperature over large domains where the contributions of the finer temperatures changes in small regions are neglected, the coarse mesh is the ideal choice. The coarse mesh allows the user to save more than 4 times to computation time needed for the simulation without loosing much in precision.

If the local temperature is required to be monitored very closely, the extra precision offered by the super-fine mesh might be necessary in exchange for a considerable longer simulation time.

8 Results

In the following section, the case studies focus on a 10-second time frame during which the doors remain open, corresponding to the estimated time for an individual to enter the building. The temperature analysis was conducted in the main hall of the BC building, approximately at the midpoint between the entrance and exit. This location was selected as it provides the most representative measurement of the interior temperature.

8.1 Case 1 : Consecutive doors

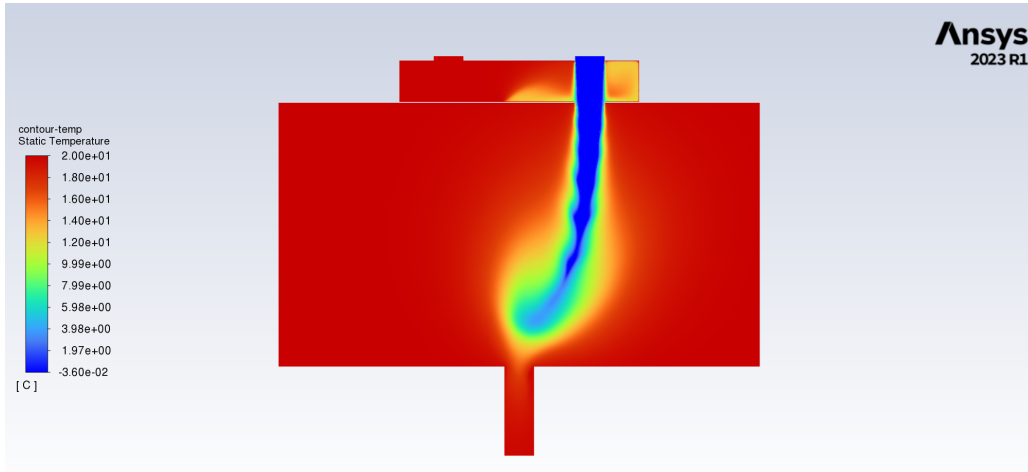


Figure 15: Case 1 : Consecutive doors (10 seconds) - Final results.

In this case, a time step of $t = 0.01$ s was utilized over a 10-second duration to study the propagation of cold air into the BC building following the opening of two consecutive doors. As illustrated in Figure 15, the cold air flows smoothly into the building, subsequently dispersing into the main hall.

Upon examining the temperature evolution presented in Figure 17, it is observed that the mid-point temperature begins to decrease after 4 seconds, rapidly dropping to 5°C before stabilizing around 11°C. This swift decline followed by stabilization can be attributed to the efficient distribution of incoming airflow throughout the main hall (see Figure 27 in the appendix §9.4). It is evident that the external temperature has a rapid and significant impact on the interior temperature. Ultimately, the temperature at the midpoint decreases by nearly half after one person enters the building through consecutive doors. This substantial temperature drop may explain the implementation of diagonal doors during winter months. This hypothesis will be further validated in the following section, which examines the impact of diagonal door configurations on interior temperature.

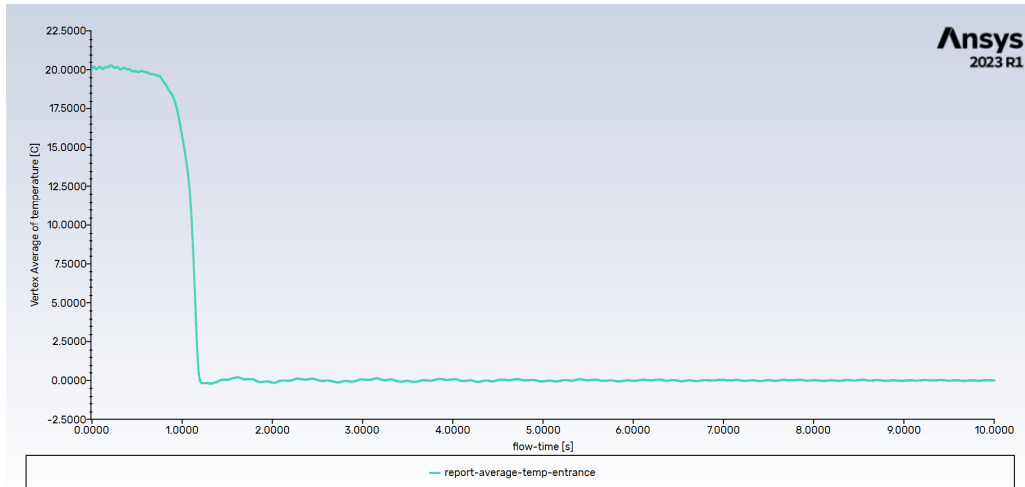


Figure 16: Case 1 : Consecutive doors - Entrance temperature evolution.

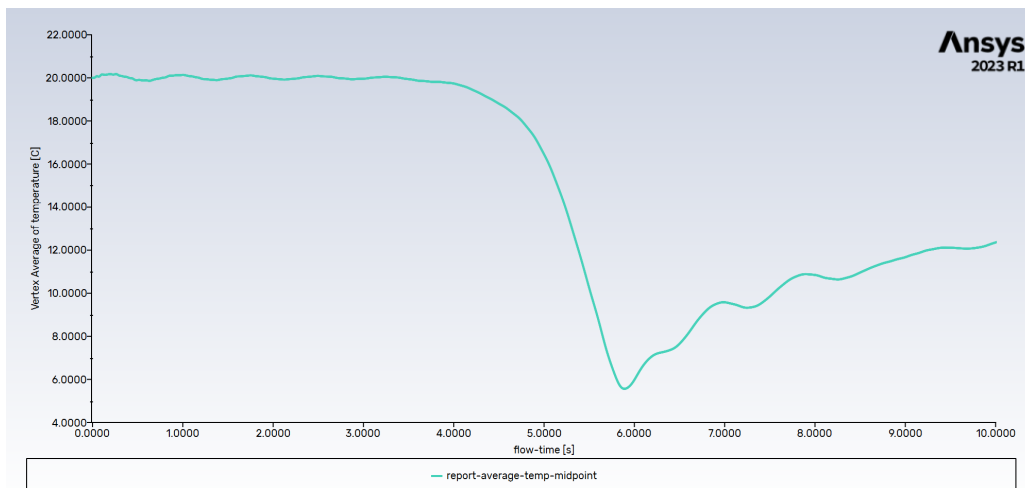


Figure 17: Case 1 : Consecutive doors - Midpoint temperature evolution.

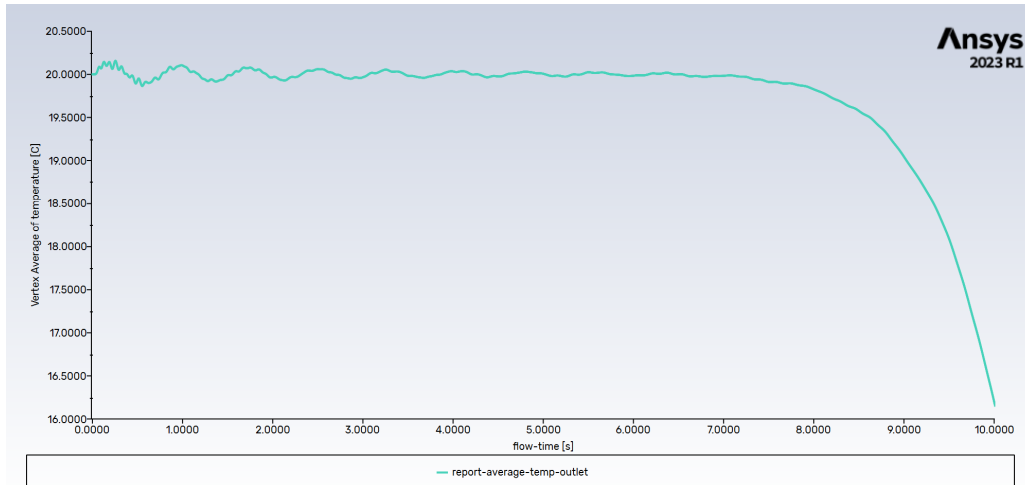


Figure 18: Case 1 : Consecutive doors - Outlet temperature evolution.

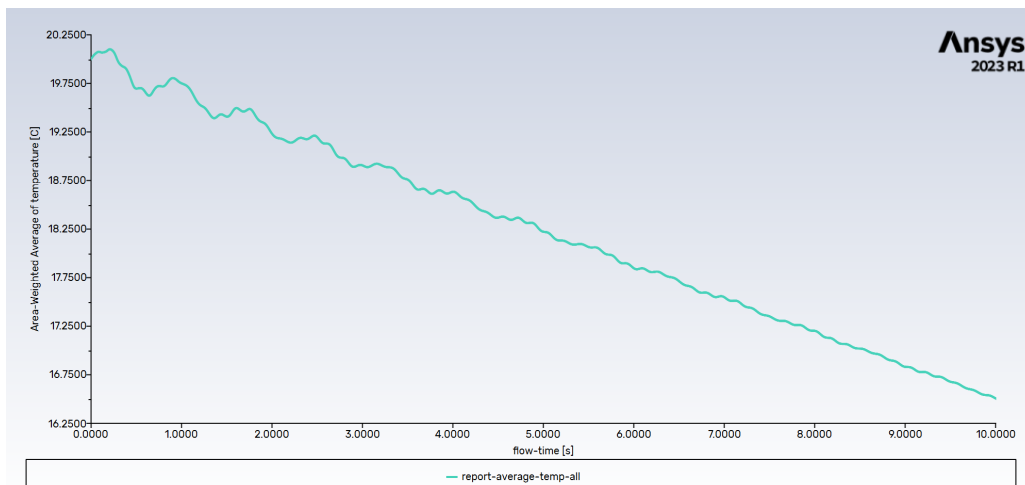


Figure 19: Case 1 : Consecutive doors - Average temperature evolution.

8.2 Case 2 : Diagonal doors.

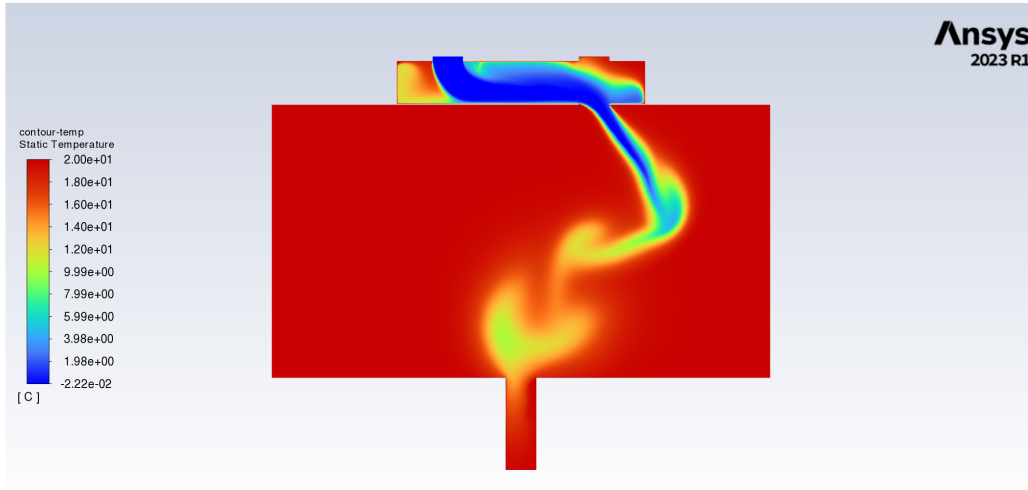


Figure 20: Case 2 : Diagonal doors (10 seconds) - Final results.

In this case, a time step of $t = 0.01\text{ s}$ was employed over a 10-second duration to analyze the propagation of cold air into the BC building with diagonal doors. As shown in Figure 20, the incoming airflow encounters significant resistance and remains largely confined to the entrance hall. This is expected, as the diagonal door configuration effectively impedes the airflow from entering the main hall.

The temperature evolution, depicted in Figure 22, reveals a distinct pattern. The midpoint temperature begins to decrease after 5 seconds, but unlike the sharp drop observed in Case 1, the decline occurs in three phases. The first phase is a gradual decrease between 5 and 7 seconds, followed by a brief stabilization between 7 and 9 seconds at approximately 18.5°C . The final phase features a more pronounced drop after 9 seconds, with the temperature settling just below 16°C . This behavior can be attributed to the airflow becoming temporarily trapped in the entry hall before eventually being drawn into the main hall, as illustrated by the airflow velocity profile in Figure 28 (refer to the appendix, §9.4).

The benefits of the diagonal door configuration are evident. Not only is the final temperature after 10 seconds significantly higher compared to the consecutive door case, but the temperature evolution is also more gradual. It can be concluded that the diagonal configuration mitigates the impact of entering airflow on the main hall's temperature, confirming its superior temperature efficiency and validating the hypothesis.

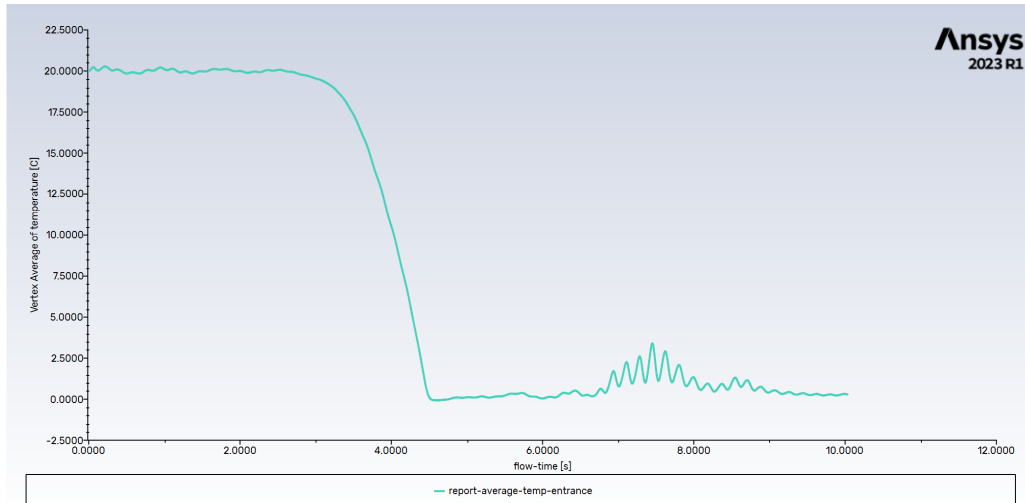


Figure 21: Case 2 : Diagonal doors - Entrance temperature evolution.

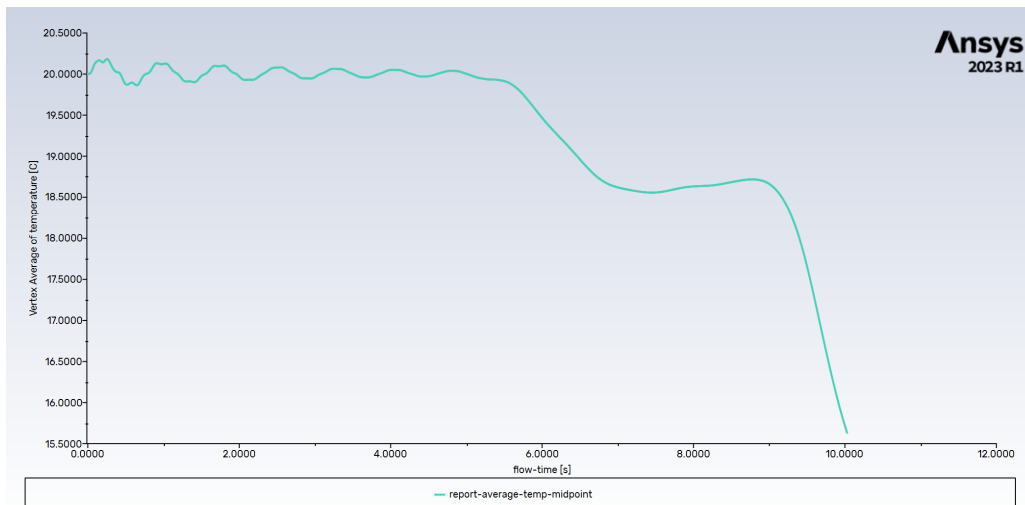


Figure 22: Case 2 : Diagonal doors - Midpoint temperature evolution.

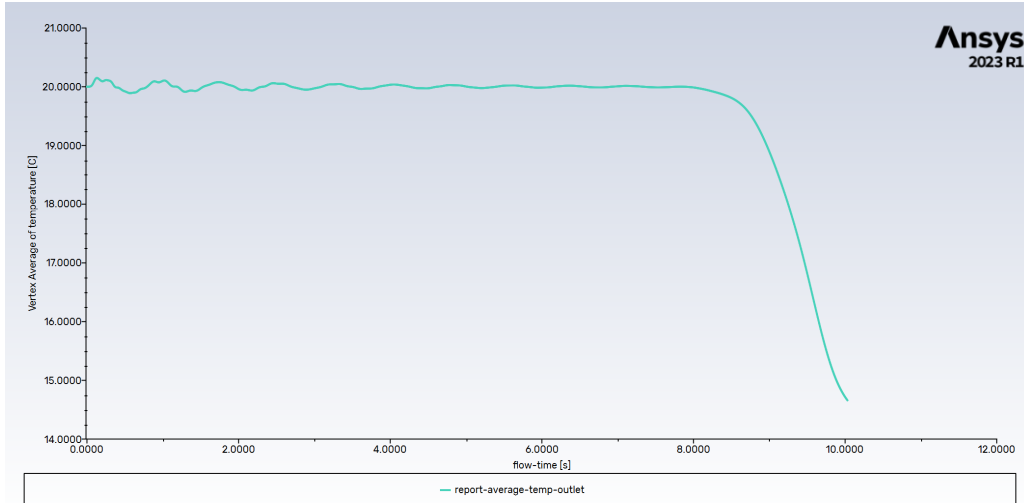


Figure 23: Case 2 : Diagonal doors - Outlet temperature evolution.

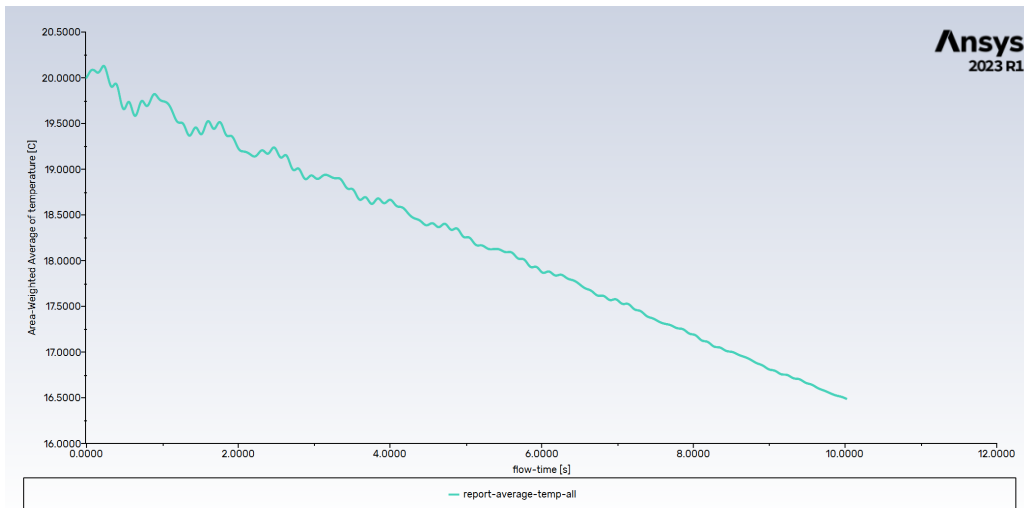


Figure 24: Case 2 : Diagonal doors - Average temperature evolution.

By comparing Figure 19 and Figure 24, we observe that the average temperature evolution is almost identical in both cases, which makes sense from an energetic point of view. The efficiency of the diagonal configuration is due to the repartition of the temperature as mentionned earlier: for the consecutive doors most of the cold air enters into the main room, while for the diagonal ones it stays in the entrance hall.

In the case of the consecutive doors, the entrance temperature (see Figure 16) makes a steep drop to 0 °C after 1 second and it stabilises there for the rest of the simulation. For the diagonal configuration, we observe that it takes 4 seconds for the temperature to drop to 0 °C, because of the greater distance between the doors (see Figure 21). The oscillations that are observed around the 7-second mark are due to the creation of vortices that cross the entrance point alternatively (see 7.6). From Figure 23 and Figure 18, we deduce that the evolution at the outlet is pretty much the same in both cases with the sole difference being the stabilisation at

15 °C for the diagonal case, while for the consecutive one we did not let the simulation run long enough to find out where the drop would stabilise.

9 Analysis & conclusions

9.1 Summary of calculated results

Summary of results	
Case 1 : consecutive doors (10s)	
Initial building temperature [°C]	20
Final building temperature [°C]	11
Case 2 : diagonal doors (10s)	
Initial building temperature [°C]	20
Final building temperature [°C]	16

Table 8: Summary of results

The final result are showing a difference of 5° in only 10 seconds, demonstrating the effect of the diagonal doors.

9.2 Relevance / accuracy of the results?

First, we had to make some approximation on the range of temperature, chosen arbitrary such as it is 0°C outside and 20°C inside. We made the same approximation on the value of the wind velocity, 3[m/s].

Then, we haven't applied any special treatment to elements close to walls, even though the mesh size should be smaller to better capture the boundary layer.

9.2.1 Comment on the minimum temperature

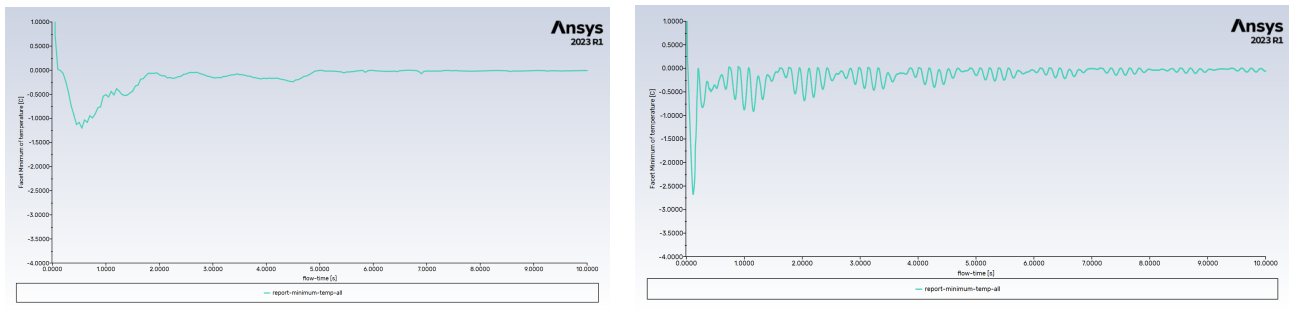


Figure 25: Impact of Δt on the minimum temperature over the whole domain (Coarse mesh).

In Figure 26a, we observe a highly oscillatory behavior at the beginning of the calculation which we would expect to disappear when using a smaller time-step, but it gets even more oscillatory for $t = 0.005$. Similarly, we obtain a quasi-identical result when also making the mesh finer in Figure 26. How can these oscillations and drops to nonphysical negative temperatures be explained ?

The most probable explanation is that while central-differencing is accurate in diffusion-dominated problems, it lacks numerical dissipation, which makes it unsuitable for advection-dominated flows. This is testified by the fact that we have a high Peclet number ($\text{Pe} \approx 490 > 2$). A remedy to that could have been to use a first-order upwind scheme, or even better, TVD (Total Variation Diminishing) schemes which blend high-order accuracy with boundedness, and is therefore better adapted to capture steep gradients.

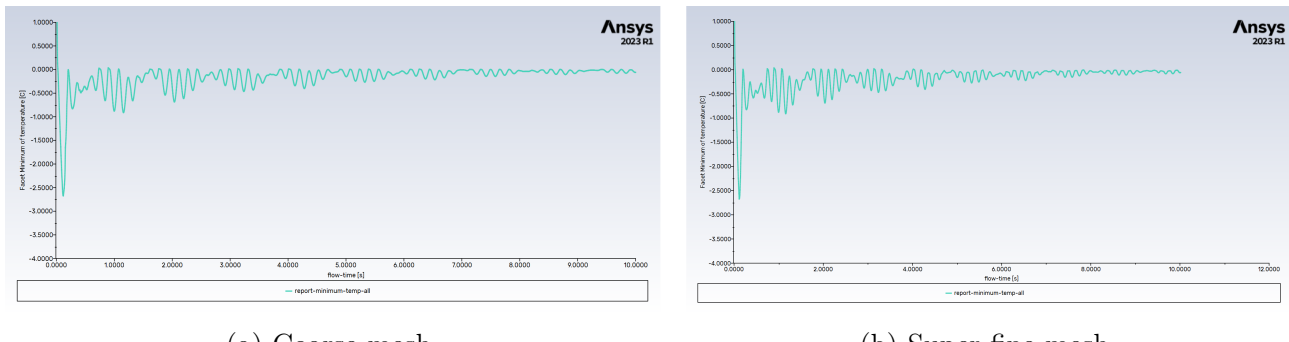


Figure 26: Impact of the mesh size on the minimum temperature over the whole domain ($\Delta t = 0.005$ s).

9.3 Conclusion

The initial question of this case study can be restated as follows:

Does the choice of door configuration significantly impact temperature and heat loss inside the building?

As demonstrated in §8, both configurations lead to a temperature drop; however, the influence of the diagonal doors is evident. The temperature decrease is less pronounced and occurs more gradually. This analysis confirms that the choice of door configuration has a tangible impact on temperature regulation and heat loss within the building. Implementing diagonal doors during winter is therefore a logical solution to maintain a higher indoor temperature and minimize energy loss, ensuring a comfortable environment for occupants.

When looking at Figure 19 and Figure 24 and comparing both plots for the average temperature inside the building, both graphs closely match. This is to no surprise as the same amount of energy is injected inside the system in both cases. The total simulation time of 10 seconds does not give enough time to the air flow to exit the domain through the hallway at the back of the building in both cases. Nevertheless, one key difference is how the temperature is spread out in the domain. In the parallel door case, the cold air flow penetrates more rapidly the main hall while the cold air flow stays trapped inside the entrance for a longer period of time.

9.4 Recommendations

The simulated case does not account for the heaters installed within the building, which are designed to maintain a constant temperature by reheating the space. These heaters are strategically positioned near the entrance to counteract the impact of incoming airflow. It can be reasonably assumed that their presence further mitigates the temperature drop. Incorporating this effect into the simulation could enhance the accuracy of the results.

However, for the purposes of this case study, sufficient data has been gathered to reliably address the research question, as the heaters influence both scenarios in a similar manner.

Furthermore, the convergence analysis was conducted using data from a single point at a specific time in the simulation. To obtain a more comprehensive understanding of mesh convergence, it would have been beneficial to analyze multiple points across different time intervals.

It could also have been interesting to use a TVD scheme to counter the oscillatory behavior at the beginning of the simulation.

Appendix

Results

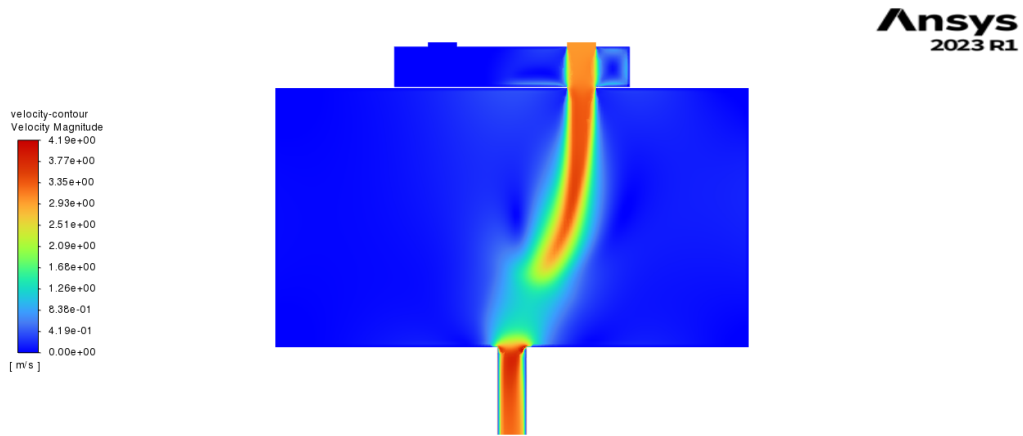


Figure 27: Case 1 : Consecutive doors (10 seconds) - Velocity

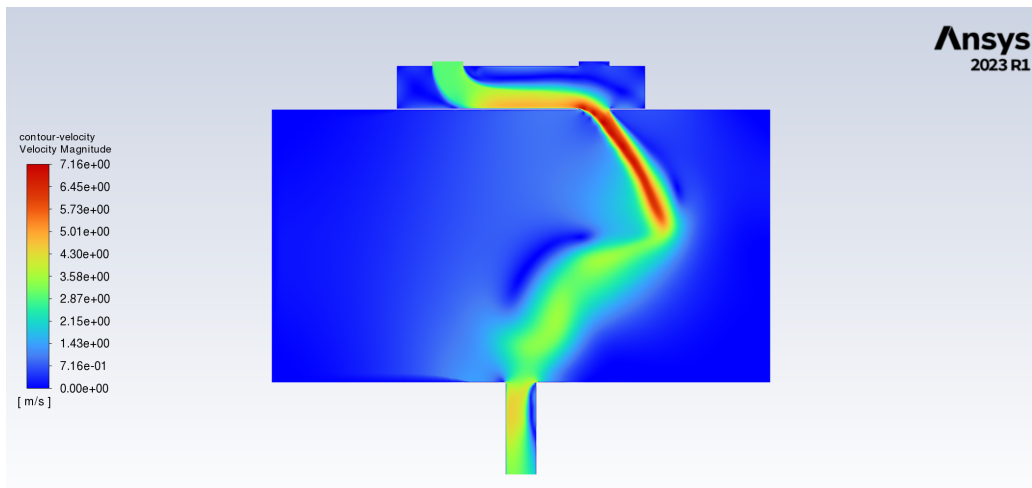


Figure 28: Case 2 : Zig zag doors (10 seconds) - Velocity

References

- [1] E. Boujo, ME-474: Numerical flow simulation, EPFL, Fall 2024.
- [2] ANSYS Inc, Ansys Fluent 2021 R2 Theory Guide, July 2021.